Multi-fingered Tactile Feedback from Virtual and Remote Environments

Alexander Kron Günther Schmidt

Instituted of Automatic Control Engineering

Technische Universität München

D-80290 München, Germany

Alexander.Kron@ei.tum.de

Abstract

This paper outlines a novel approach of displaying multi-fingered tactile feedback information from remote and virtual environments. Miniature tactile fingertip modules are developed allowing multi-fingered integration into an already existing hand force exoskeleton for display of combined tactile and kinesthetic feedback. The tactile feedback comprises generation of both, vibrotactile and thermal stimuli directly at the operator's fingertip where a multitude of human tactile receptors are located. The proposed parallel configuration of integrated vibration and heat display with combined kinesthetic feedback actuators considers a novel approach towards the generation of holistic haptic sensations. Corresponding tactile rendering algorithms are presented computing realistic tactile stimuli of object properties from either remote real or virtual environments. Moreover, the article discusses the design of a developed thermal and texture sensor with corresponding data processing algorithms for online identification of tactile object properties in a remote environment. The new quality of generated multi-fingered tactile feedback was evaluated in several experiments enabling a human operator performing exploratory tasks.

1 Introduction

The design of advanced interactive systems enabling a human operator (HO) executing exploratory and manipulatory tasks in virtual (VE) and remote (RE) environments requires *multimodal feedback* [6, 11]. Typical applications are tele-surgery, tele-assembly, simulation and training systems. Today, the interaction in an environment is performed over a human-system interface (HSI) equipped with integrated multimodal feedback actuators (see Fig. 1), each related to one of the human senses: vision, audition, kinesthesia, touch, smell and taste. While highly developed 3D visualization techniques and auditory feedback systems are already commercially available, the design of advanced haptic feedback systems is still in a rather early stage of development.

Typically humans are accustomed to execute exploratory or manipulatory tasks by using their hands and fingers [11]. Hand and finger kinematics comprise many degrees of freedom ensuring a high level of skillfulness and dexterity. The sensitiveness of the human hand is based on a multitude of neural receptors embedded inside the fingertips. Humans are experienced in using this permanently available tactile and kinesthetic information in an intuitive manner. The assumption underlying our work is that intuitive and more proper task execution in VEs or REs requires similar haptic feedback. In this context, the design of multi-fingered haptic feedback displays play a key role.
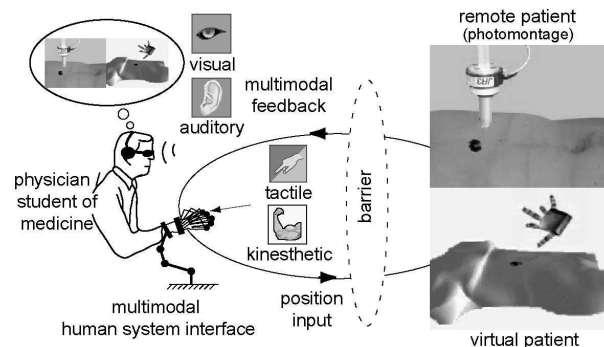

Figure 1. Telediagnosis: an application for an advanced interactive system with multimodal feedback.

In spite of a considerable progress in the design of exoskeleton-based multi-fingered kinesthetic feedback displays [2, 14], there is still a lack of integrated tactile feedback components. However, additional tactile feedback would augment various applications - e.g. palpation of a virtual patient in a medical training system or palpation of a remotely located patient via a telediagnosis system (see. Fig. 1). A physician diagnosing for example skin diseases will require beside visual and auditory feedback *combined* kinesthetic and tactile information of several haptic submodalities - e.g. texture, thermal and stiffness feedback. State-of-the-art tactile feedback displays already ensure high feedback quality, but often only for a *single sub-*

modality and *single-fingered* display [5, 8]. Corresponding bulky hardware set-ups prohibit multi-fingered extension as well as the desired system integration into hand kinesthetic feedback devices. Concerning heat and vibration feedback several single-fingered displays have been developed [9, 13] as well as first multi-fingered tactile feedback gloves with either embedded vibrotactile *or* thermal actuators [4, 7]. An overall *parallel configuration* of a multi-fingered *kinesthetic* feedback display combined with integrated *vibrotactile and heat* fingertip display has not been realized up to now.

This paper outlines a design for this type of multi-fingered haptic feedback display, based on integrating *miniature modular* tactile fingertip devices into an exoskeleton-based kinesthetic feedback glove. The tactile feedback enables generation of vibrotactile and thermal stimuli directly at the operator's fingertip. The paper presents the design of the developed tactile fingertip feedback modules and describes corresponding algorithms for tactile feedback computation. Contrary to experiencing VEs, teletaction in REs requires in addition online identification of remote tactile object properties. The article outlines novel designs of tactile sensors and implemented data processing algorithms for remote data acquisition and identification of texture and thermal properties. The proposed methods allow the generation of high fidelity tactile feedback interacting with both VEs as well as REs. The new quality of displayed multi-fingered feedback was evaluated in several experiments.

The paper is organized as follows: Section 2 outlines the hardware set-up of recently developed tactile fingertip modules. Section 3 reports on tactile feedback computation algorithms. Section 4 describes sensor design and methods for tactile data acquisition in REs. Experimental results of the multi-fingered tactile feedback generation from REs and VEs are finally discussed in Section 5.

2 Tactile Fingertip Feedback Modules

Multi-fingered tactile sensation is achieved by the design of tactile fingertip feedback modules - called TactTip modules (see Fig. 2a). The midget fingertip devices produce vibrotactile and thermal stimuli [10] at an operator's fingertip.

Vibrotactile feedback is generated by means of a miniaturized DC-motor with a freewheeling out of balance mass at top of the motor shaft (see Fig. 2b). With a maximum speed of 10.000 RPM the vibration motor produces vibratory frequencies up to about 166 Hz with amplitudes > 3 μm. This type of vibrotactile feedback stimulates Pacini as well as Meissner's corpuscles embedded in the human fingertip [3] and ensures noticeable vibrotactile sensation. The vibration motor is controlled by an adjustable motor current as input. Amplitude and frequency of the vibratory output are coupled by a fixed relation.
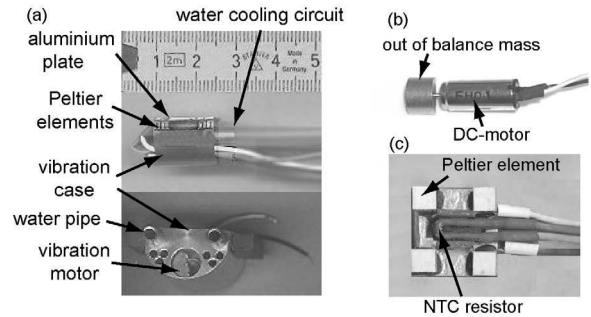

Figure 2. Tactile fingertip feedback module.

The additional *temperature feedback* display comprises 4 serially connected Peltier elements producing cold as well as hot temperatures. Fig. 2c illustrates the tiny elements with a size of 4x4x2.3 mm^3. The display achieves heating and cooling rates of +4.0 K/s and -2.5 K/s, respectively, and generates temperatures over the range from 8°C to 80°C. For safety reasons the highest output temperature is limited to 42°C. The Peltier elements are mounted on a small-sized aluminium plate (10x15x0.5 mm^3) together with a standard NTC resistor measuring the displayed temperature for heat control. This plate ensures optimal thermal contact with the human fingertip. The overall temperature display is clipped onto a specially designed vibration case, embedding the freewheeling vibration motor. Since Peltier elements are only capable of producing temperature differences between both sides of an element, generation of a low temperature at the displaying side is directly accompanied by heat development on the opposite side. To avoid such heating a miniaturized water cooling circuit is integrated into the module (see Fig. 2a). The miniature size of the presented TactTip modules ensures the multi-fingered system integration into an exoskeleton-based kinesthetic feedback display as demonstrated by Fig. 3 [10].
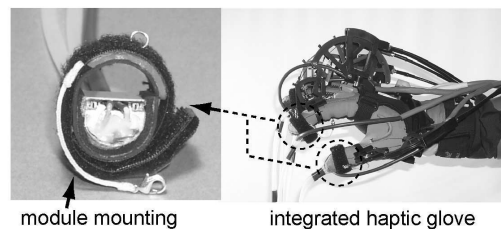

Figure 3. Integration of TactTip modules in a hand force feedback exoskeleton.

3 Tactile Feedback Computation

Beside the physical generation of tactile stimuli, rendering algorithms are required for computing stimuli which ensure realistic vibrotactile and thermal sensations. Implemented feedback computation algorithms applied to the TactTip modules are described next.

3.1 Computation of Vibrotactile Stimuli

Display of vibrotactile stimuli ensures perception of texture and object surface properties [9, 12]. Typical vibratory actuator components - e.g. piezoceramics, voice coil speakers - are controlled by the common vibratory parameters: amplitude, frequency, and damping [12]. With respect to a miniature actuator design ($< 10x15x3$ mm^3) these actuators produce vibratory stimuli too weak to be perceived in addition to strong finger forces up to 10 N. In our approach midget vibration motor ensures generation of noticeable stimuli. For this purpose the motor only provides 2 vibratory control parameters: amplitude and damping of motor rotation speed, while amplitude and frequency of the vibratory output are coupled by a fixed relation. However, experiments with the vibration motor have led to the following hypothesis: *"A vibration motor controlled by means of individual rendering algorithms can provide the HO with vibrotactile feedback comprising expected information content"*. This type of feedback can be fused by the HO to realistic sensations ensuring differentiation of various surface textures.

The implemented vibrotactile rendering algorithms take into account a bias component as well as additional damped impulses of motor rotation speed for producing the desired vibration feedback. As typical exploratory procedures [11] the algorithms distinguish *tapping at* and *stroking over* an object surface. *Tapping* means that either the fingertip collides with an object surface for a short time or it remains fixed on the surface after a tap. At any rate the algorithm displays a damped vibration impulse for a constant time interval T_t (see Fig. 4). The generated tapping impulse is damped by an exponential decay of the corresponding motor rotation speed $A_t(t)$. First $A_t(t)$ is set to a fixed attack amplitude A_o, which is made proportional to the HO's tapping velocity v_n normal to the object surface multiplied by an object specific constant value $K_{v,t}$, Eq.(1). The corresponding damping coefficient B_t also depends on the object material.

$$A_o(v) = K_{v,t} \cdot v_n \qquad (1)$$

Stroking means, that the HO's fingertip slides with the velocity $v_s(t)$ and the contact force $F_n(t)$ over an object surface. Typically vibration stimuli are perceived stronger by increasing $v_s(t)$ or $F_n(t)$ [12]. During stroking the amplitude $A_s(t)$ of the motor speed is set proportional to both $v_s(t)$ and $F_n(t)$ with material specific coefficients $K_{v,s}$ and $K_{F,s}$, i.e.

$$A_s(v(t), F(t)) = K_{v,s} \cdot v_s(t) + K_{F,s} \cdot F_n(t) \qquad (2)$$

Eq.(2) shows that stroking over object surfaces with homogenously distributed texture is displayed by a bias component of the motor speed, depending on $v_s(t)$ or $F_n(t)$ (see Fig. 4). Vibrotactile perception of patterned objects is realized by adding damped impulses $J(t)$ to $A_s(t)$. Such an added impulse has a constant offset amplitude A_J with again an object specific damping coefficient B_J.

The proposed vibrotactile feedback computation algorithms are applied for interaction in VEs as well as REs. Results of experiments comparing displayed vibration feedback from VEs with stimuli sensed by using the human hand in a real physical environment are presented in Section 5.1.
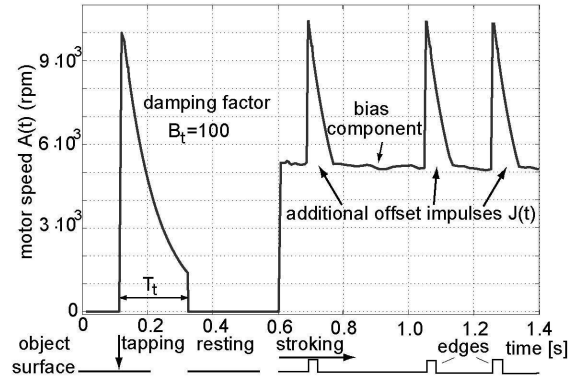

Figure 4. Motor rotation speed while tapping and stroking over an object surface.

3.2 Computation of Thermal Stimuli

For display of realistic thermal stimuli heat transmission phenomena need to be considered [1]. Note, that the HO's temperature perception differs while exploring varying materials with equal surface temperature as caused by object specific heat conductivities. The human temperature perception is mainly affected by a dynamic temperature distribution inside the fingertip where human thermoreceptors are embedded. The proposed thermal rendering algorithms use a corresponding dynamical model determining the temperature distribution inside the fingertip during two significant exploratory modes:

- free fingertip motion in 3D space without object contact,

- fingertip contact with objects.

In the model the human fingertip tissue is decomposed into 3 cutaneous layers: epidermis, dermis, and endodermis. For each layer the gain in heat accumulation dQ/dt per cm^2 is given by

$$\frac{dQ}{dt} = \Delta x \rho c \frac{dT}{dt} \qquad (3)$$

where Δx is the thickness of a layer, ρ is the density of the cutaneous layer, c is the specific heat and dT/dt is the temperature change rate. Heat exchange between adjacent layers is modelled by

$$\phi(t) = \frac{K_{(n+1,n)}}{\Delta X_{(n+1,n)}} [T_{n+1} - T_n] \qquad (4)$$

where $K_{(n+1,n)}$ is the thermal conductivity between the center of both layers $n+1$ and n, $\Delta X_{(n+1,n)}$ is the distance between these centers, and T_n is the individual temperature

of a layer [1]. The model assumes heat flow through all layers to be in normal direction and neglects lateral heat flow. The heat flow between endodermis and dermis is affected by additional heat flows from fat tissue and blood vessels. Dynamical parameters like metabolism and the arterial blood temperature are here assumed to be constant for feedback computation.

Fig. 5 illustrates the overall scheme of the implemented thermal feedback computation. In a first stage the temperature distribution inside the fingertip for an individual contact in an environment is computed by ordinary differential equations, leading to a three-layered ODE-model. These equations require initial temperature values of the tissue layers $\boldsymbol{T}^0$ as well as parameter vectors $\boldsymbol{\theta}_i$, comprising specific thermal parameters of the tissue layers and virtual objects. The ODE-model provides T_1^s, representing the temperature of the first tissue layer. Note, that we assume human skin receptors for thermal perception to be located in this layer. Fig. 6 depicts the simulated temperature distribution caused by heat flow through all three layers for fingertip contact at objects out of iron and wood (surface temperature 35°C) after free fingertip motion (environmental temperature 25°C).
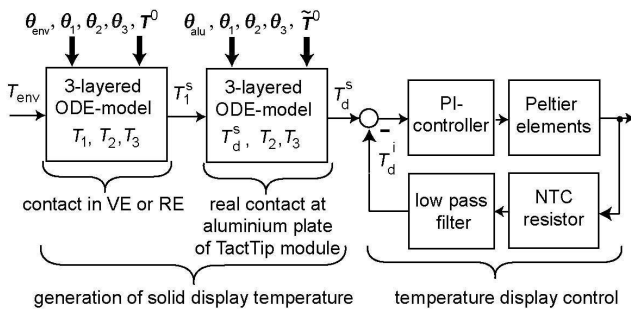

Figure 5. Scheme of thermal feedback computation.

A second three-layered ODE-model simulates the fingertip contact with the real aluminium plate of the TactTip module. T_1^s from the first ODE-model enables the computation of a solid display temperature T_d^s, whose display leads to the desired T_1^s inside the physical HO's fingertip. A temperature control loop controls the thermal feedback device. Experimental results, reported in Section 5.1, demonstrated that the proposed rendering algorithms ensure the sensation of realistic thermal object properties during exploration in VEs or REs.

4 Tactile Data Acquisition

The proposed rendering algorithms for tactile feedback generation with the TactTip modules are applied to task execution in VEs as well as in REs. Interaction with a VE only requires specifying individual rendering parameters,

---

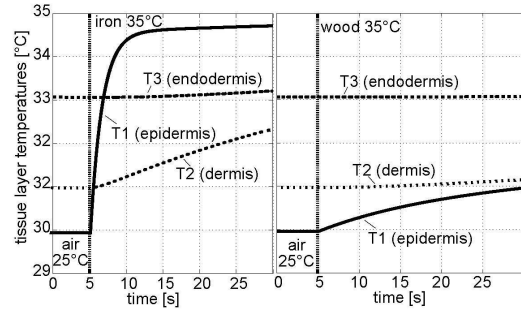[1]Specific thermal characteristics of these 3 cutaneous layers are presented in [10].

Figure 6. Simulated temperature distribution for fingertip contact at iron and wood.

like e.g. surface roughness, heat conductivity, etc. On the other hand object interaction in a RE requires online tactile data acquisition by means of tactile sensors. Data processing algorithms must compute corresponding texture and thermal rendering parameters by identifying remote object properties from measured data. Developed sensor designs as well as appropriate data processing algorithms are described next.

4.1 Texture Measurement

Measurement of texture information in a RE is achieved by means of a developed miniaturized texture sensor based on the piezoelectric effect (see Fig. 7). The sensor device comprises 2 small-sized piezoceramics ($\emptyset$ 10 mm) pasted together with a cone-shaped tip made out of steel. During object surface exploration the miniature tip of the sensor transmits pressure signals to the piezoceramics for transformation into voltage signals. Theses signals are integrated, low pass filtered and amplified. Pressure inputs up to 10 N generates output signals up to 10 V. The 12 bit A/D converted pressure signals are employed for identification of the object surface roughness.
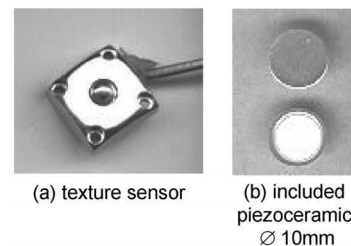

Figure 7. Sensor design for texture measurement.

Section 3.1 has already demonstrated that the proposed computation of vibrotactile stimuli requires a multitude of object and task specific parameters. The corresponding parameter identification is achieved by fusing sensor data available from the remote telemanipulation system. Fig. 8 outlines an overall scheme of sensor data fusion and data processing.
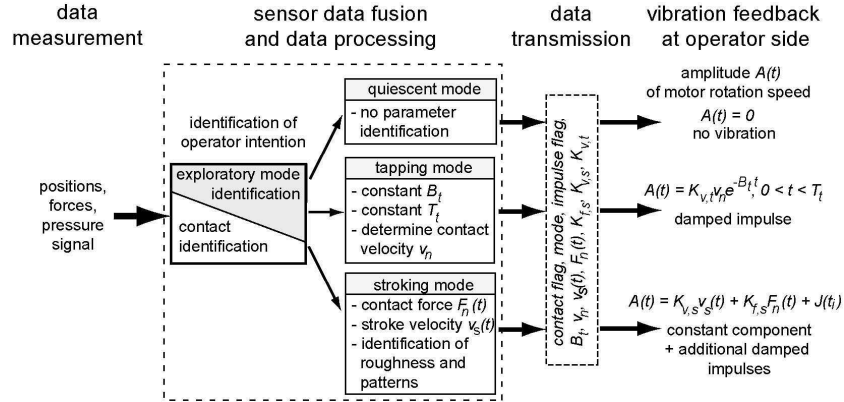
Figure 8. Scheme of vibrotactile parameter identification in RE.

Telemanipulation systems are typically equipped with position and force sensors. Corresponding available sensor data as well as measured texture data are inputs for the vibrotactile parameter identification algorithm. A measured contact force normal to an object surface characterizes contact with the object. In addition the operator's intention of exploring the object's surface needs to be determined. At any rate the first contact with an object surface results in displaying a damped impulse characterized by the *tapping mode*. If the HO rests after a tap with the endeffector of the telemanipulator on the surface, no vibration feedback is expected. The *quiescent mode* is identified if stroke velocities are less than a threshold value or the HO did not move a certain minimum distance from the tapping point. If the operator motion exceeds the determined distance by a minimum stroke velocity, the algorithm identifies the *stroking mode*. The mode identification returns to quiescent mode, if the HO looses object contact or rests again on the surface.

During the short time period of a tap an identification of an object material is not feasible. In this case, required object specific parameters B_t and $K_{v,t}$ are determined by heuristics. They are considered constant for each displayed damped impulse. Thus vibratory stimuli displaying a tap only vary because of different normal contact velocities.

While stroking over a surface, the stroke velocity as well as the contact force are derived from position and force sensor data. The parameters $K_{v,s}$ and $K_{f,s}$ are identified by approximating the actual roughness of an object surface using the time discrete pressure signal p_k, which is measured by the texture sensor presented above. The implemented data processing algorithm computes absolute values $\tilde{p}_k$, Eq.(5) and an average value $\bar{p}_k$, Eq.(6) at each time-step k.

$$\tilde{p}_k = |p_k| \qquad (5)$$

Note, that $\bar{p}_k$ is always evaluated as an average value over all $k = 1..i$ discrete time-steps belonging to an actual stroking procedure.

$$\bar{p}_k = \frac{\sum_{k=1}^{i} \tilde{p}_k}{i} \qquad (6)$$

$K_{v,s}$ and $K_{f,s}$ are defined by classification of computed $\bar{p}_k$. If $\bar{p}_k$ shows a value inside a heuristically chosen interval, the required parameters are determined. The corresponding intervals for the output parameter values $K_{v,s}$ and $K_{f,s}$ are also chosen heuristically.

Stroking over patterned structures, e.g. grooves or edges, at a discrete time-step $k = j$ is identified by a value $\tilde{p}_j$ much greater than actual computed $\bar{p}_j$. In this case the algorithm sets an impulse flag. High pressure signals $\tilde{p}_k$ ($k > j$) caused by stroking over the patterned structure influence computation of the next time-discrete $\bar{p}_k$ values. However, the algorithm requires $\bar{p}_k$ values as reasonable estimates of the common surface roughness neglecting sporadic patterns. Thus the algorithm computes next $\bar{p}_k$ values ($k > j$) using the stored $\tilde{p}_j$ value instead of actual $\tilde{p}_k$ values until stroking over the patterned structure is finished. If actual $\tilde{p}_k$ falls below a threshold close to $\bar{p}_j$, the end of the patterned structure is detected. From here $\tilde{p}_k$ values are again used for computing $\bar{p}_k$ at succeeding time-steps. The presented algorithm is appropriate for generating a reasonable estimate for the required object surface roughness.

Section 5.2 outlines results demonstrating that measured and computed vibrotactile parameters generate vibratory stimuli enabling the HO to distinguish between varying object surfaces in a RE.

4.2 Thermal Parameter Identification

The challenge of identifying thermal parameters in a RE is attached by determining the current surface temperature as well as material specific parameters, e.g the heat conductivity. While miniature temperature sensors measuring the object surface temperature with short time delays are commercially available, tiny sensors determining heat conductivity of a material are still lacking. However, this parameter is required for the previously presented thermal rendering algorithms. We designed a novel miniature thermal sensor based on the thermal contact model depicted in Fig. 9.

Let us assume a thermal sensor component with an embedded heat source which is coming into contact with a remote object as a heat sink. Neglecting all lateral heat flow,

the remaining heat flow in normal direction is computed by

$$\phi = \frac{A(T_s - T_o)}{\Delta x_s/\lambda_s + \Delta x_o/\lambda_o} \qquad (7)$$

with the contact area A, the temperatures T_s, T_o, the conductivities λ_s, λ_o, and the thicknesses $\Delta x_s, \Delta x_o$. For online thermal parameter identification the parameters $A, T_s, \lambda_s, \Delta x_s$ are known. Since ϕ cannot be measured, we introduce C as a *virtual heat capacity* for describing the dispensed sensor heat Q by

$$\phi = C\frac{dT_s}{dt} = \frac{dQ}{dt} \qquad (8)$$

Inserting Eq.(7) into Eq.(8) leads to the ODE:

$$\frac{dT_s}{dt} = \alpha\frac{A}{c}(T_s - T_o) \qquad (9)$$

with

$$\alpha = \frac{\Delta x_s}{\lambda_s} + \frac{\Delta x_o}{\lambda_o} \qquad (10)$$

Its solution is given by

$$T_s(t) = (T_s^0 - T_o^0)e^{-(\alpha/C \cdot At)} + T_o^0 \qquad (11)$$

with the initial temperatures T_s^0, T_o^0 at the beginning of a thermal contact.

thermal sensor (λ_s, T_s)

heat source

heat flow

Δx_s

Δx_o

heat sink

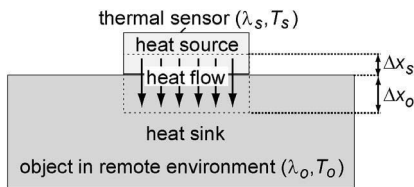object in remote environment (λ_o, T_o)

Figure 9. Contact model for heat flow in RE.

If the design of a device producing the proposed type of modelled heat flow during object contact is possible, extrapolation of the measured temperature data allows to predict the exponential response of $T_s(t)$, see Eq.(11). A corresponding prediction algorithm determines the virtual heat conductivity term α/C as well as the steady state temperature $T_s(t \to \infty)$, which is equal to the actual object surface temperature T_o^0. However, because of several simplifying assumptions concerning the modelled heat flow, the predicted α/C is not the exact material specific heat conductivity. It represents a virtual parameter ensuring a classification of known remote object materials. Thus, the proposed algorithm allows an online material identification. Subsequently, demanded object specific thermal parameters are determined using a look-up table.

Fig. 10 illustrates the developed thermal sensor design. It comprises a small-sized case (14x14x8 mm^3) made out of PVC with two separated chambers. In the first chamber a standard silizium spread resistor (SSR) is embedded for temperature measurement. The second chamber is filled by a miniaturized Peltier element (4x4x2.3 mm^3). Both actuator and sensor components are coupled with a thin aluminium plate as top of the sensor.

The integrated Peltier element enables heating of the aluminium plate. If no contact between telemanipulator and objects is detected, the temperature of the aluminium plate is closed loop controlled to a defined offset temperature compared with environmental temperature[2]. If an object contact is detected, the controlled sensor heating is switched off and the embedded SSR measures $T_s(t)$ required for the proposed prediction algorithm. 5-8 seconds after a contact the implemented algorithm is capable of generating reasonable values for the actual object surface temperature as well as the virtual heat conductivity used for material identification. Results of this thermal online parameter identification procedure are presented in Section 5.2
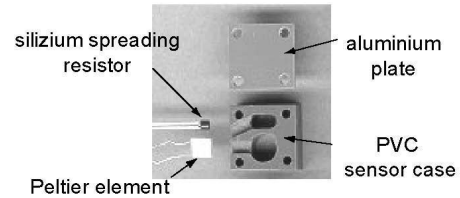

silizium spreading resistor

aluminium plate

Peltier element

PVC sensor case

Figure 10. Sensor design for temperature and heat conductivity measurement in RE.

5 Experimental Results

The following two subsections outline experimental results of generated thermal and vibrotactile feedback from VEs and REs.

5.1 Object Identification Experiments

The quality of displayed tactile feedback was evaluated in object identification experiments. Virtual scenarios were developed for testing texture identification by vibrotactile feedback as well as the capability of generating realistic thermal sensations. In these experiments additional kinesthetic feedback on fingers and wrist was applied. The corresponding test objects were both implemented in a VE and were also available as real components.

For a *texture exploration experiment* three object surfaces - sandpaper, foam and plain PVC - were selected providing homogeneously distributed surface textures. Other test objects with patterned textures were grooved PVC blocks (see Fig. 11a). Virtual objects were visualized with the same optical appearance (see Fig. 11b), but they differed with respect to surface properties. The subjects were assigned the task to match the virtual objects with their real equivalent. Additionally, each of the subjects rated the quality of perceived haptic stimuli from 1 (*unrealistic*) up to 5 (*realistic*). For this rating the virtual objects were visualized with the textured optical appearance as depicted in Fig. 11c. One result of the experiment (see Table 1) was that surfaces with homogenous texture were more difficult to identify than grooved objects.

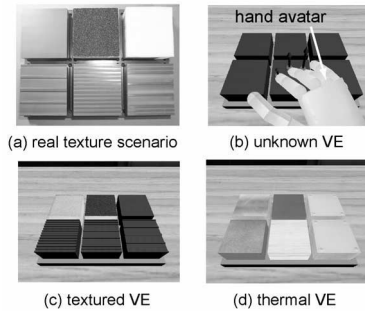[2]The environmental temperature in RE is measured by a separate temperature sensor.

Figure 11. Real and virtual scenarios.

Note, that we implemented all objects with same stiffness for kinesthetic feedback display. This caused difficulties for the subjects to distinguish between the foam and the plain PVC object. This experiment proved that subjects were capable to identify varying surface textures by the displayed vibratory stimuli. Moreover, the experiment demonstrated that subjects were capable of fusing parallel displayed tactile and kinesthetic stimuli to overall haptic perceptions. However, if haptic stimuli were not consistent - like e.g. displaying foam with too high stiffness - fusion of perceived stimuli was disturbed.

surface	matching [%]	rating	
		$\bar{x}$	σ
foam	60	2.45	0.9945
sandpaper	90	2.7	0.9579
plain PVC	70	3.6	0.9894
grooved PVC			
closely	90	3.55	0.6863
arbitrarily	85	3.65	0.8751
widely	85	3.85	0.7452

Table 1. Results of 20 novice haptic feedback users matching real and virtual objects.

For *thermal exploration experiments* objects made out of aluminium (a), ceramic (c), PVC (p) and wood (w) were again available as real components and were implemented as VE with same surface temperatures. Subjects were assigned to explore respectively two different virtual as well as physical object materials (see Fig. 11d), based on their thermal perception. The results demonstrated a satisfactory accordance between the exploration of objects in the VE and in the real world as depicted in Table 2. In both cases, materials with relatively similar heat conductivity such as PVC and wood turned out to be harder to distinguish, whereas significant differences in thermal conductivity were perceived reliably. The experiment substantiated the conclusion still achieved from the texture exploration scenario, that subjects were able to fuse the simultaneously displayed tactile and kinesthetic stimuli.

5.2 Remote Data Acquisition

The efficiency of the earlier presented texture sensor and the capability of implemented data processing algorithms

obj.	real [%]			virtual [%]		
1-2	$1 < 2$	$1 = 2$	$1 > 2$	$1 < 2$	$1 = 2$	$1 > 2$
a-p	100	0	0	100	0	0
c-w	91.7	8.3	0	83.3	16.7	0
a-c	91.7	0	8.3	91.7	0	8.3
p-w	41.7	58.3	0	66.7	33.3	0

Table 2. Results of 12 novice haptic feedback users exploring two objects with different thermal properties.

to identify online required parameters for vibrotactile feedback computation were tested in a single-fingered remote scenario (see Fig. 12). Fig. 12a illustrates a RE with varying textured objects as well as the telemanipulator carrying the endeffector equipped with the texture sensor (see Fig. 12b).
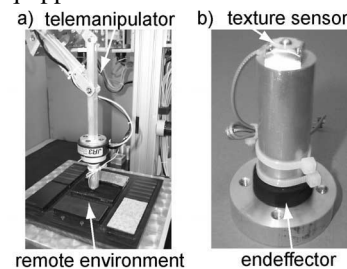

Figure 12. Texture sensing in RE.

At the operator site subjects were enabled to explore remote objects by means of a hand force exoskeleton combined with one TactTip module located at the index fingertip. The subject's task was to identify different object surfaces by performing a stroking procedure. The results proved that the texture sensor and implemented data processing algorithms allowed the identification of homogenously textured surfaces with differing roughness. Subjects were also able to assert the sensation of patterns, e.g. grooves and edges, on corresponding surfaces. The online identified vibratory parameters led to a satisfactory quality of vibrotactile feedback which the HO fused to realistic haptic sensations.

The capability to identify thermal parameters in REs were tested using the presented thermal sensor for touching varying object materials with similar surface temperatures. Fig. 13 illustrates predicted results of the object surface temperature as well as of the virtual heat conductivity touching an aluminium object. The time responses show that the prediction algorithm generates 7 seconds after contact satisfactory predicted values for both thermal parameters T_s^0, T_o^0. The implemented algorithm allows identification of the object material by means of classification using the evaluated virtual heat conductivity. The subsequent parameter determination using a look-up-table of known materials in RE ensures transmission of reliable thermal parameters to the operator site a short time period after a surface contact. With these parameters the computation of realistic thermal feedback for display with the TactTip module

is made possible. Subjects asserted the sensation of different thermal sensations touching objects with differing heat conductivities but similar surface temperatures in the RE.
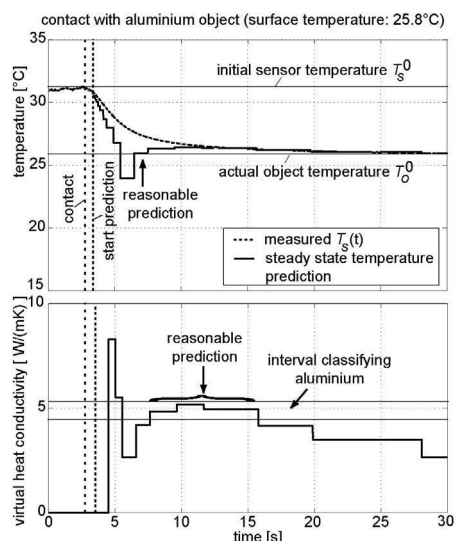

Figure 13. Results of thermal parameter identification in RE.

6   Conclusions

This paper outlined a methodology and experimental results for display of multi-fingered haptic feedback from VEs and REs taking into account the combined display of *heat, vibration* and *kinesthetic* feedback. The proposed hardware set-up is based on a hand force exoskeleton equipped with miniature tactile fingertip devices. The article presented the design of novel TactTip modules generating desired vibrotactile as well as thermal stimuli. Moreover, we reported on tactile rendering algorithms for generation of vibrotactile and thermal stimuli with the TactTip module ensuring realistic sensation of thermal object properties and surface textures. For the interaction with REs novel sensor designs and data processing algorithms were developed. The efficiency of the proposed methods for displaying multi-fingered tactile feedback from REs and VEs was demonstrated in several exploratory experiments. The results proved that operators were capable of fusing parallel haptic stimuli of various submodalities into overall haptic perceptions. We consider the proposed extended haptic glove system a novel approach towards the generation of *holistic haptic sensations*. We are convinced that this type of combined tactile and kinesthetic feedback display will be key for task execution in advanced VE and RE applications, as for example the above mentioned palpation scenario of virtual or remote patients. We expect that this new quality of haptic sensations will increase the operator's degree of immersion into corresponding environments and will support a proper and more intuitive operator's task execution.

References

[1] M. Bergamasco, A. A. Alessi, and M. Calcara. Thermal Feedback in Virtual Environments. *Presence*, 6(6):617–629, December 1997.

[2] M. Bouzit. *Design, Implementation and Testing of a Data Glove with Force Feedback for Virtual and Real Objects Telemanipulation*. PhD thesis, Laboratoire de Robotique de Paris, 1996.

[3] G. Bruggencate. Allgemeine Physiologie sensorischer Systeme. In P. Deetjen and E. J. Speckmann, editors, *Physiologie*, pages 43–55. Schwarzenberg, Oldenburg, 1994.

[4] D. Caldwell, N. Tsagarakis, and A. Wardle. Mechano Thermo and Proprioceptor Feedback for Integrated Haptic Feedback. In *Proc. of IEEE Int. Conf. on Robotics and Automation*, pages 2491–2496, 1997.

[5] V. Hayward and J.-M. Cruz-Hernandez. Tactile Display Device using Distributed Lateral Skin Stretch. In *Proc. of the Ninth Annual Symposium on Haptic Interfaces for Virtual Environment and Teleoperator Systems*, pages 1309–1314, Orlando, FL, 2000.

[6] J. Hollerbach. Some Current Issues in Haptics Research. In *Proc. of the IEEE Int. Conf. on Robotics and Automation*, pages 757–762, 2000.

[7] Immersion, Corp. Tactile feedback man-machine interface device. An United States Patent, no.: 6,088,017 http://www.immersion.com, 2000.

[8] P. Kammermeier, A. Kron, and G. Schmidt. Towards intuitive multi-fingered haptic exploration and manipulation. In *Proc. of the Workshop on Advances in Interactive Multimodal Telepresence Systems*, pages 57–70, München, March 2001.

[9] D. A. Kontarinis and R. D. Howe. Tactile Display of Vibratory Information in Teleoperation and Virtual Environments. *Presence*, 4(4):387–402, 1995.

[10] A. Kron and G. Schmidt. Multi-fingered Haptic Feedback from Virtual Environments by means of Midget Tactile Fingertip Modules. In *Proc. of the 8th Mechatronics Forum International Conference*, pages 1191–1200, University of Twente, Netherlands, 2002.

[11] S. Lederman and R. Klatzky. Designing Haptic and Multimodal Interfaces: A Cognitive Scientist's Perspective. In *Proc. of the Workshop on Advances in Interactive Multimodal Telepresence Systems*, pages 71–80, München, March 2001.

[12] A. M. Okamura, J. T. Dennerlein, and R. D. Howe. Vibration Feedback Models for Virtual Environments. In *Proc. of the IEEE International Conference on Robotics and Automation*, pages 674–679, Leuven, Belgium, 1998.

[13] M. P. Ottensmeyer and J. K. Salisbury. Hot and Cold Running VR: adding thermal stimuli to the haptic experience. In *Proc. of the 2nd PHANDToM User's Group Workshop, AI Lab Technical Report 1617*, pages 34–37, 1997.

[14] M. Turner, D. Gomez, M. Tremblay, and M. Cutkovsky. Preliminary Tests of an Arm-Grounded Haptic Feedback Device in Telemanipulation. In *Proc. of the Winter Annual Meeting of ASME'98*, volume 64, pages 145 – 149, Nov. 1998.